

Ground-state properties of the O(2) lattice model in two dimensions: A correlated-basis-function approach

Khaled Abu Qasem*

*Max-Planck Institut für Physik komplexer Systeme, D-01187 Dresden, Germany*M. L. Ristig[†]*Institut für Theoretische Physik, Universität zu Köln, D-50937 Köln, Germany*

(Received 31 October 2003; published 20 August 2004)

We study the ground-state properties of the O(2) model for a system of spin-1 rotors on a simple square lattice. We assume that the rotors interact via nearest-neighbor forces, the coupling characterized by a strength parameter λ . This many-boson model can be physically realized, for example, through a two-dimensional configuration of Josephson junction arrays or superfluid ^4He in confined geometries. The formal and numerical analysis of the model concentrates on a study of the strong correlations induced by the interactions. The theoretical investigation is performed within a semianalytic *ab initio* approach employing the theory of correlated basis functions, on the variational level. In the past the formalism has been successfully applied for quantitative analyses of spatial correlations in quantum fluids. In the present work it is formally adapted for treating the O(2) model. We express the ground-state energy by an appropriate functional in terms of the reduced on-site density profile and of the site-site distribution function. Employing the familiar minimum principle for the ground-state energy we construct two associated Euler-Lagrange equations which determine the optimal correlated ground-state of Hartree-Jastrow type. We present solutions of these equations and numerical results on various ground-state properties as functions of the coupling strength λ . We discuss in detail the behavior of the density profile and of the site-site distribution function. We also report data on the order parameter for the symmetry-broken ordered phase and on the critical strength λ_c for the transition to the disordered phase.

DOI: 10.1103/PhysRevB.70.085106

PACS number(s): 71.10.Fd, 05.30.-d, 05.50.+q, 67.40.Db

I. INTRODUCTION

The O(2) lattice model¹ is of theoretical interest in quantum statistical physics² and as a suitable model to study phase transitions in a number of interesting materials exhibiting order-disorder phenomena.³ For instance, it may be interpreted as a model for an array of interacting quantum rotors.⁴ Its Hamiltonian consists of two noncommuting terms: a potential energy representing the coupling between two-component spin vectors of unit length and a kinetic energy term that takes account of the rotational degrees of freedom of the rotors. As a second example, we may adopt the O(2) model to describe the physics of Josephson junction arrays (JJAs)^{5,6} or granular superconductors^{7,8} which are composed of superconducting islands or grains coupled by Josephson junctions. Such nets can be manufactured⁹ with different geometries where the junction parameters can be varied experimentally, at least to some extent. Another physical realization of the model is liquid ^4He in restricted geometries such as porous glasses,¹⁰ where the potential energy may represent a discretized form of the gradient energy term in the Ginzburg-Landau free energy of superfluid ^4He favoring a state in which all parts of the superfluid have the same condensate phase, while the kinetic energy term arises from the time variation of the order parameter, i.e., from the phase coherence.

At nonzero temperatures the behavior of the O(2) model is governed by the interplay between thermal and quantum fluctuations.¹¹ At very low temperatures the model still dis-

plays a rich behavior due to the competition between the kinetic energy portion and the potential energy contribution, where quantum fluctuations of the rotor angle play the most important role.¹² For such a behavior the quantity of the system is measured by a coupling parameter λ , whose value depends on the relative weight of kinetic and potential energy parameters. Of particular interest are therefore the properties of the correlated ground state of the model which depend strongly on the strength of the coupling factor that determines the magnitude of the quantum fluctuations. Depending on the value λ the rotors may more or less align and may form an ordered phase with spin-wave-like excitations. In contrast, the rotor orientations may be disordered in another coupling regime where the ground states are eigenstates of zero total angular momentum and the excitations are quasiparticles. The order parameter characterizing the quantum phase may be formally interpreted as a spontaneous magnetization (or nonzero angular momentum). If the model describes a system of JJAs the physical interpretation is: we have an ordered superconducting phase or a disordered insulating phase with a superconductor/insulator phase transition¹³ at a critical value of the coupling parameter. In this case the order parameter should be better called a condensate fraction. Most of the theoretical studies on the O(2) model have used perturbation theory, mean-field theory,^{5,14} or the harmonic approximation.^{12,15} Mean-field calculations¹⁶⁻¹⁹ have given strong evidence that the system in two spatial dimensions does not become ordered for $\lambda \geq 4.0$ and for $\lambda \geq 6.0$ in three spatial dimensions. However,

these methods ignore or do not take sufficient account of the strong site-site correlations and can therefore only provide qualitative descriptions. Some studies explored the correlation effects by using perturbation expansions in powers of the coupling strength λ ,²⁰ employed renormalization-group theory,² approximate numerical simulations,^{21,22} or quantum-spherical approximations.²³ The latter method gives a value $\lambda_c \approx 2.43$ for the critical coupling. Thus, the correlations lower significantly the critical coupling strength $\lambda_c \approx 4$ derived in mean-field approximation.^{5,13} Perturbation theory truncated at third order predicts instead a value²⁰ $\lambda_c \approx 2.52$. To achieve an accurate enumeration of the critical data or, more generally, a quantitatively reliable study of the existing strong correlation effects as functions of the coupling strength one should therefore refine these approaches or resort to other more powerful treatments.

In the present work we study the correlation effects within the framework of the correlated basis function (CBF) theory.^{24,25} This powerful *ab initio* approach has been successfully employed in many quantitative studies of strongly correlated many-body systems, notably homogeneous and inhomogeneous quantum fluids, but also lattice gauge models and spin lattices.^{26–28}

After a brief qualitative description of the O(2) model in mean-field approximation our investigation within the CBF theory begins with the construction of a correlated ground-state energy functional with respect to a set of trial many-body states of Hartree-Jastrow type. In this context, we note that the CBF theory may be viewed as a generalization of the familiar energy density-functional theory where the energy functional depends on the density profile. In the CBF theory the functional depends not only on the density but also on the site-site distribution function (more generally, on the elements of the reduced two-body density matrix). Therefore, the CBF approach could be adequately characterized as a pair-density functional theory. To find the best trial wave function of Hartree-Jastrow type we apply the familiar minimum principle for the CBF ground-state energy functional. The optimization procedure generates two Euler-Lagrange equations. They can be interpreted as a renormalized Hartree equation for the one-body (on-site) density profile and as a renormalized Schrödinger equation for the two-body (site-site) correlation function. To connect the latter quantity with the correlated trial ground-state wave function we perform a hypernetted-chain (HNC) analysis that leads to a coupled set of HNC equations. Ignoring the so-called elementary components (HNC/0 approximation) yields a closed set of HNC equations that provides an explicit expression for the relation between the trial state and the corresponding reduced density-matrix elements. Within this realization of the CBF theory numerical calculations are performed on the optimal on-site density and the optimal site-site distribution function of the O(2) model. We then analyze in detail the solutions of the Euler-Lagrange equations and calculate and discuss the results on the optimal ground-state energy, the optimal order parameter, and the critical coupling strength.

In Sec. II we introduce the main features of the adopted O(2) model. We summarize briefly some mean-field results in Sec. III, which are necessary to start the application of the CBF theory for a quantitative investigation of correlation

effects (Sec. IV). In Sec. V we report and discuss the results of our microscopic calculations on the optimal correlated ground-state properties, in particular, on the one-body and two-body densities, the energy, and the order parameter. The final section summarizes the results and concludes with an outlook on further applications, extensions, and improvements (Sec. VI). The Appendix collects some information on the numerical procedure.

II. MODEL DESCRIPTION

The quantum O(2) model defined on a d -dimensional spatial lattice is a special case ($n=2$) of the general chiral O(n) lattice model.²⁹ Its dynamic behavior is stored in the Hamiltonian¹⁶

$$H = -\lambda \sum_i^N \frac{\partial^2}{\partial \varphi_i^2} + \frac{1}{2} \sum_{i,j}^N \Delta_{ij} \cos(\varphi_i - \varphi_j), \quad (1)$$

where i and j refer to lattice sites. The sum extends over N lattice points characterized by the set of phase angles (operators) $\{\varphi_i\}$ with $-\pi \leq \varphi_i \leq \pi$. Correlations between the phases on the lattice are induced by the two-body (site-site) potential $v_0(\mathbf{n}; \varphi_i, \varphi_j) = \Delta(\mathbf{n}) \cos(\varphi_i - \varphi_j)$ where $\Delta(\mathbf{n}) = \Delta_{ij}$ measures the strength of the correlations and depends on the relative distance $\mathbf{n} = \mathbf{r}_i - \mathbf{r}_j$. For simplicity, we assume a simple square lattice and a short-ranged interaction, setting $\Delta(0) = 4$, $\Delta(\mathbf{n}) = -1$ for the four nearest neighbors, $\Delta(\mathbf{n}) = 0$ otherwise. The differential operator $-i \partial / \partial \varphi_i$ ($\hbar = 1$) is the canonical conjugate operator to the phase variable φ_j . It may be interpreted as the number operator of excited quanta, the number of Cooper pairs in JJAs, of the free field operator $-\partial^2 / \partial \varphi_j^2$. The parameter λ ($0 \leq \lambda \leq \infty$) is the coupling parameter that can be experimentally varied (to some extent) in the case of granular superconductors. For these materials the strength parameter is determined by the ratio $\lambda = 4U/J$ with the charging energy U and the Josephson coupling J .

If the strength λ is small, the system exhibits a second-order quantum phase transition at sufficiently low temperatures, at a critical coupling λ_c separating the ordered phase from the disordered phase. The transition occurs because of Heisenberg's uncertainty principle expressed by the commutation relation $[-i \partial / \partial \varphi_i, \varphi_j] = -i \delta_{ij}$. For small values of λ the kinetic energy term is small compared to the coupling potential that tends to make the individual phases φ_j coherent on a macroscopic scale. In contrast, for large values of λ the operator $-i \partial / \partial \varphi_i$ has well defined eigenvalues and the phase φ_j is completely uncertain. This leads to sufficiently large quantum phase fluctuations which destroy the long-range order of the system. While the disordered ground states conserve the symmetries of the Hamiltonian (1), the O(2) rotational symmetry (and the chiral symmetry) is broken under the transformations $\{\varphi_i \rightarrow \pi - \varphi_i\}$ in the ordered phase. The symmetry violation may be measured by the order parameter

$$M_x = \langle \Psi | \cos \varphi_1 | \Psi \rangle / \langle \Psi | \Psi \rangle \quad (2)$$

defined as an expectation value with respect to the ground state of the system (or by a thermal average at nonzero temperatures).

III. MEAN-FIELD THEORY

In order to get a qualitative view of the model properties and to prepare the ground for starting the CBF theory we employ mean-field theory in this section. This simple approach ignores, of course, correlation effects from the outset. The many-body states of the Hamiltonian (1) are approximated by a product of unit normalized single-particle (on-site) states of the form

$$\Psi(\varphi_1, \varphi_2, \dots, \varphi_N) = \prod_i^N \psi(\varphi_i). \quad (3)$$

The mean-field Hamiltonian is obtained by replacing the coupling term between two lattice sites in the original Hamiltonian by an averaged interaction involving only single-site operators. We thus approximate

$$\frac{1}{2} \sum_{i,j}^N \Delta_{ij} \cos(\varphi_i - \varphi_j) \rightarrow 2d \langle \cos \varphi \rangle \sum_i^N \cos(\varphi_i), \quad (4)$$

where d is the dimension of the system ($d=2$ in the present study). The Hamiltonian (1) is therewith replaced by a sum of single-site hamiltonians, with eigenfunctions $\psi_n(\varphi)$. They can be determined from the Hartree equation

$$H_{MF}^i \psi_n(\varphi_i) = - \left(\lambda \frac{\partial^2}{\partial \varphi_i^2} + 2d M_x \cos \varphi_i \right) \psi_n(\varphi_i) = e_n \psi_n(\varphi_i). \quad (5)$$

Given the solutions $\psi_n(\varphi)$ and their eigenvalues e_n to Eq. (5) the order parameter $M_x(\lambda, T)$ and the energy per site $E(\lambda, T)/N$ at temperature T can be calculated self-consistently from the relations

$$M_x = \langle \cos \varphi \rangle = \frac{\sum_n^{\infty} e^{-\beta e_n} \langle \psi_n | \cos \varphi | \psi_n \rangle}{\sum_n^{\infty} e^{-\beta e_n}}, \quad (6)$$

$$E/N = \langle H_{MF}^i \rangle = \frac{\sum_n^{\infty} e^{-\beta e_n} \langle \psi_n | H_{MF}^i | \psi_n \rangle}{\sum_n^{\infty} e^{-\beta e_n}}, \quad (7)$$

with $\beta=1/k_B T$. At zero temperature only the ground-state eigenfunction contributes to the sums in Eqs. (6) and (7). In this case the ground-state energy per site is given by

$$E_0/N = -\lambda \langle \psi_0 | \frac{\partial^2}{\partial \varphi^2} | \psi_0 \rangle + d(1 - M_x^2), \quad (8)$$

where $M_x = \langle \psi_0 | \cos \varphi | \psi_0 \rangle$. Straightforward minimization of this functional yields the optimal solution $\psi_0(\varphi) = \text{constant}$ for the disordered phase with $M_x=0$ and constant energy $E=2N$. The optimal wave function $\psi_0(\varphi)$ of the ordered phase is a solution of the Hartree equation

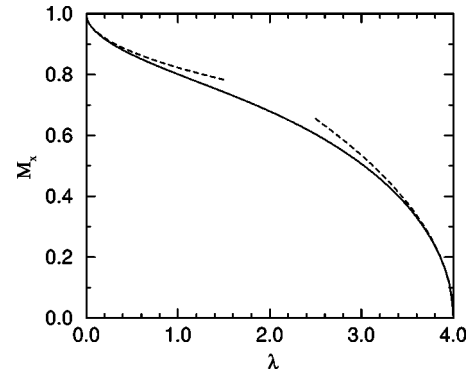


FIG. 1. Numerical results on the optimal order parameter $M_x(\lambda)$ for the ordered phase, in mean-field approximation ($0 \leq \lambda \leq \lambda_c=4$). Dashed lines show the results of perturbation theory in lowest order, Eqs. (10) and (11) for $\lambda \rightarrow 0$ and $\lambda \rightarrow \lambda_c^-$, respectively.

$$- \left(\lambda \frac{\partial^2}{\partial \varphi_i^2} + 2d M_x \cos \varphi_i \right) \psi_0(\varphi_i) = e_0 \psi_0(\varphi_i). \quad (9)$$

Equation (9) is essentially a differential equation of the familiar Mathieu type that can be easily solved by a standard iteration procedure. Figures 1 and 2 display numerical results, respectively, on the order parameter and the minimum ground-state energy as functions of the coupling strength λ , in mean-field approximation.

At $\lambda=0$ the system is exactly described by mean-field theory because phase correlations are absent and the ordering is perfect. Function $\psi_0(\varphi)$ is proportional to a delta function $\delta(\varphi)$, the order parameter M_x is unity, and the ground-state energy E is zero. For increasing values λ the ordering decays gradually and disappears completely at the (mean-field) critical value $\lambda_c=4$. The energy per lattice site increases monotonously in the ordered phase until the coupling strength $\lambda_c=4$ is attained. The results merge smoothly with the constant energy value $E=2N$ of the disordered phase. In the limit $\lambda \rightarrow 0$ low-order perturbation theory yields the correct results

$$M_x = 1 - \frac{1}{8} \sqrt{2\lambda}, \quad E/N = \sqrt{2\lambda}. \quad (10)$$

They are well reproduced by the numerical mean-field results for sufficiently small parameter values λ . For $\lambda \rightarrow \lambda_c$

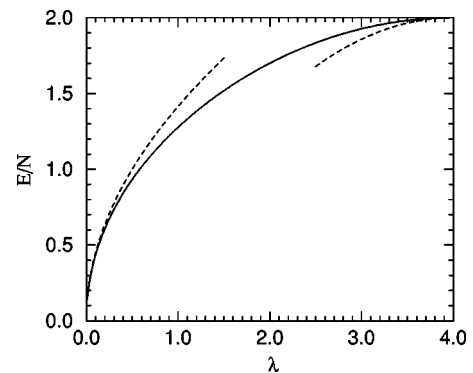


FIG. 2. Ground-state energy per lattice site E/N as function of coupling parameter λ , results in mean-field approximation. Dashed lines indicate results of perturbation theory, Eqs. (10) and (11) in lowest order for $\lambda \rightarrow 0$ and $\lambda \rightarrow \lambda_c^-$, respectively.

=4 the solutions of Eq. (9) in the ordered regime yield the analytic behavior

$$M_x \cong \sqrt{\frac{2}{7}(\lambda_c - \lambda)}, \quad E/N \cong 2 - \frac{1}{7}(\lambda_c - \lambda)^2. \quad (11)$$

In the asymptotic regime $\lambda \rightarrow \infty$ of the disordered phase the rotor-rotor (site-site) interactions may be ignored and the problem can be exactly solved. Elementary perturbation expansion in powers of λ^{-1} gives for the energy per site

$$E/N \cong 2 - \frac{1}{2\lambda} + \dots. \quad (12)$$

The results already indicate that correlation effects are most important in the transition region $\lambda \approx \lambda_c$. For analyzing the properties of these correlations and their influence on the second-order phase transition we may employ modern quantum many-body theories or stochastic procedures.

IV. BEYOND MEAN-FIELD: CORRELATIONS

To analyze the phase correlations in the ground state of the O(2) model as functions of the strength λ we employ the CBF theory on the variational level. A reasonable form for the correlated ground state is provided by the Hartree-Jastrow ansatz^{30,31}

$$|\Psi\rangle = \Lambda \exp\left\{\frac{1}{4}\sum_{i \neq j}^N u(\mathbf{n}_{ij}; \varphi_i, \varphi_j)\right\} |\Psi_0\rangle, \quad (13)$$

where Λ is a normalization factor chosen such that $\langle \Psi | \Psi \rangle$ equals unity and $|\Psi_0\rangle$ is a symmetric product of N unit-normalized single-site states. The function $u(\mathbf{n}; \varphi_i, \varphi_j)$ is the phase-dependent pseudopotential defined on the lattice sites i and j . It must fulfill the subcondition

$$\frac{1}{2\pi} \int_{-\pi}^{\pi} d\varphi_2 \rho(\varphi_2) u(\mathbf{n}; \varphi_1, \varphi_2) = 0. \quad (14)$$

At this stage we introduce two physical quantities which provide us with the relevant information on the phase correlations on the lattice. These are the on-site density and the site-site reduced density matrix elements. For the O(2) model with a translationally invariant lattice ground-state $|\Psi\rangle$ they are defined by

$$\rho(\varphi_1) = \frac{1}{(2\pi)^{N-1}} \int_{-\pi}^{\pi} \dots \int_{-\pi}^{\pi} d\varphi_2 \dots d\varphi_N \Psi^2(\varphi_1, \varphi_2, \dots, \varphi_N), \quad (15)$$

$$\rho(\varphi_1)\rho(\varphi_2)g(\mathbf{n}; \varphi_1, \varphi_2) = \frac{1}{(2\pi)^{N-2}} \int_{-\pi}^{\pi} \dots \int_{-\pi}^{\pi} d\varphi_3 \dots d\varphi_N \times \Psi^2(\varphi_1, \varphi_2, \dots, \varphi_N). \quad (16)$$

In mean-field approximation the probabilities (15) and (16) specialize, of course, to $\rho(\varphi_1) = \psi_0^2(\varphi_1)$ and the uncorrelated product $\rho(\varphi_1)\rho(\varphi_2)$, respectively. The correlations contribute implicitly to quantity (15) and explicitly to the conditional probability (16) via the site-site distribution function

$g(\mathbf{n}; \varphi_1, \varphi_2)$ that may strongly deviate from unity. We may calculate the expectation value of the ground-state energy with respect to the selected set (13) and express the result as a functional in terms of quantities (15) and (16). It may be cast into the form³¹

$$E/N = 2 - \lambda \frac{1}{2\pi} \int_{-\pi}^{\pi} d\varphi_1 \sqrt{\rho(\varphi_1)} \frac{\partial^2}{\partial \varphi_1^2} \sqrt{\rho(\varphi_1)} + \frac{1}{2} \sum_{\mathbf{n} \neq 0} \frac{1}{(2\pi)^2} \int_{-\pi}^{\pi} \int_{-\pi}^{\pi} d\varphi_1 d\varphi_2 \rho(\varphi_1)\rho(\varphi_2)g(\mathbf{n}; \varphi_1, \varphi_2) \times v^*(\mathbf{n}; \varphi_1, \varphi_2), \quad (17)$$

involving the Feenberg effective potential^{25,31}

$$v^*(\mathbf{n}; \varphi_1, \varphi_2) = v_0(\mathbf{n}; \varphi_1, \varphi_2) + \frac{\lambda}{4} [D(1) + D(2)] u(\mathbf{n}; \varphi_1, \varphi_2). \quad (18)$$

The second term in Eq. (18) is induced by the pseudopotential $u(\mathbf{n}; \varphi_1, \varphi_2)$ and involves the generating differential operator $D(\varphi_i) \equiv D(i)$ with

$$D(i) = -\frac{1}{\rho(\varphi_i)} \frac{\partial}{\partial \varphi_i} \rho(\varphi_i) \frac{\partial}{\partial \varphi_i}. \quad (19)$$

The functional (8) is recovered by specializing to the mean-field approximation, i.e., replacing the distribution function $g(\mathbf{n}; \varphi_1, \varphi_2)$ by unity and the Feenberg effective potential $v^*(\mathbf{n}; \varphi_1, \varphi_2)$ by the phase-phase interaction potential $v_0(\mathbf{n}; \varphi_1, \varphi_2)$.

An explicit relation between the pseudopotential $u(\mathbf{n}; \varphi_1, \varphi_2)$ and the site-site distribution function $g(\mathbf{n}; \varphi_1, \varphi_2)$ allows the calculation of the Feenberg effective potential $v^*(\mathbf{n}; \varphi_1, \varphi_2)$. This relation is provided by a set of coupled HNC equations.²⁷ For the O(2) model these equations are given by^{27,31}

$$X'(\mathbf{n}; \varphi_1, \varphi_2) = (1 - \delta_{\mathbf{n},0}) \{ \exp[u(\mathbf{n}; \varphi_1, \varphi_2) + N'(\mathbf{n}; \varphi_1, \varphi_2) + E(\mathbf{n}; \varphi_1, \varphi_2)] - 1 \} - N'(\mathbf{n}; \varphi_1, \varphi_2), \quad (20)$$

$$N'(\mathbf{n}; \varphi_1, \varphi_2) = \sum_{\mathbf{m}} \frac{1}{2\pi} \int_{-\pi}^{\pi} d\varphi_3 \rho(\varphi_3) X'(\mathbf{n} - \mathbf{m}; \varphi_1, \varphi_3) \times [X'(\mathbf{m}; \varphi_3, \varphi_2) + N'(\mathbf{m}; \varphi_3, \varphi_2)], \quad (21)$$

$$g(\mathbf{n}; \varphi_1, \varphi_2) = (1 - \delta_{\mathbf{n},0}) [1 + X'(\mathbf{n}; \varphi_1, \varphi_2) + N'(\mathbf{n}; \varphi_1, \varphi_2)]. \quad (22)$$

The primed quantities $X'(\mathbf{n}; \varphi_1, \varphi_2)$ and $N'(\mathbf{n}; \varphi_1, \varphi_2)$ read

$$X'(\mathbf{n}; \varphi_1, \varphi_2) = X(\mathbf{n}; \varphi_1, \varphi_2) - X(\mathbf{n}; \varphi_1) - X(\mathbf{n}; \varphi_2) + X(\mathbf{n}), \quad (23)$$

$$N'(\mathbf{n}; \varphi_1, \varphi_2) = N(\mathbf{n}; \varphi_1, \varphi_2) - N(\mathbf{n}; \varphi_1) - N(\mathbf{n}; \varphi_2) + N(\mathbf{n}), \quad (24)$$

where

$$X(\mathbf{n}; \varphi_1) = \frac{1}{2\pi} \int_{-\pi}^{\pi} d\varphi_2 \rho(\varphi_2) X(\mathbf{n}; \varphi_1, \varphi_2), \quad (25)$$

$$N(\mathbf{n}; \varphi_1) = \frac{1}{2\pi} \int_{-\pi}^{\pi} d\varphi_2 \rho(\varphi_2) N(\mathbf{n}; \varphi_1, \varphi_2), \quad (26)$$

$$X(\mathbf{n}) = \frac{1}{(2\pi)^2} \int_{-\pi}^{\pi} \int_{-\pi}^{\pi} d\varphi_1 d\varphi_2 \rho(\varphi_1) \rho(\varphi_2) X(\mathbf{n}; \varphi_1, \varphi_2), \quad (27)$$

$$N(\mathbf{n}) = \frac{1}{(2\pi)^2} \int_{-\pi}^{\pi} \int_{-\pi}^{\pi} d\varphi_1 d\varphi_2 \rho(\varphi_1) \rho(\varphi_2) N(\mathbf{n}; \varphi_1, \varphi_2). \quad (28)$$

The functions $X(\mathbf{n}; \varphi_1, \varphi_2)$, $N(\mathbf{n}; \varphi_1, \varphi_2)$, and $E(\mathbf{n}; \varphi_1, \varphi_2)$ are, respectively, the non-nodal (direct), nodal, and elementary components of the total set of diagrams that graphically represents the distribution function $g(\mathbf{n}; \varphi_1, \varphi_2)$. In the following we ignore the elementary components appearing in the HNC equations thereby adopting the so-called HNC/0 approximation [$E(\mathbf{n}; \varphi_1, \varphi_2) = 0$].

In a next step we employ the minimum principle for the ground-state energy to evaluate the optimal elements (15) and (16) and therewith the lowest value E/N . To do this, we first eliminate the function $u(\mathbf{n}; \varphi_1, \varphi_2)$ from the energy functional (17) with the aid of the HNC/0 equations and consider the one-body density $\rho(\varphi)$ and the site-site distribution function as independent variables. We further write the energy functional in the form

$$\begin{aligned} E/N = & 2 - \lambda \frac{1}{2\pi} \int_{-\pi}^{\pi} d\varphi_1 \sqrt{\rho(\varphi_1)} \frac{\partial^2}{\partial \varphi_1^2} \sqrt{\rho(\varphi_1)} \\ & + \frac{1}{2} \sum_{\mathbf{n} \neq 0} \frac{1}{(2\pi)^2} \int_{-\pi}^{\pi} \int_{-\pi}^{\pi} d\varphi_1 d\varphi_2 \rho(\varphi_1) \rho(\varphi_2) \\ & \times [g(\mathbf{n}; \varphi_1, \varphi_2) v_0(\mathbf{n}; \varphi_1, \varphi_2) + \lambda v_c(\mathbf{n}; \varphi_1, \varphi_2)]. \quad (29) \end{aligned}$$

The potential $v_c(\mathbf{n}; \varphi_1, \varphi_2)$ is induced by the correlations and is given by

$$\begin{aligned} v_c(\mathbf{n}; \varphi_1, \varphi_2) = & \sqrt{g(\mathbf{n}; \varphi_1, \varphi_2)} [D(1) + D(2)] \sqrt{g(\mathbf{n}; \varphi_1, \varphi_2)} \\ & - \frac{1}{4} g(\mathbf{n}; \varphi_1, \varphi_2) [D(1) + D(2)] N'(\mathbf{n}; \varphi_1, \varphi_2). \quad (30) \end{aligned}$$

Finally, independent variation of the pair-density functional (29) with respect to $\sqrt{\rho(\varphi)}$ and $\sqrt{g(\mathbf{n}; \varphi_1, \varphi_2)}$ generates two coupled Euler-Lagrange equations

$$\left[-\lambda \frac{\partial^2}{\partial \varphi^2} + v_d(\varphi) + v_e(\varphi) \right] \sqrt{\rho(\varphi)} = \mu \sqrt{\rho(\varphi)}, \quad (31)$$

$$\begin{aligned} [D(1) + D(2)] \sqrt{g(\mathbf{n}; \varphi_1, \varphi_2)} + [v_0(\mathbf{n}; \varphi_1, \varphi_2) \\ + w(\mathbf{n}; \varphi_1, \varphi_2)] \sqrt{g(\mathbf{n}; \varphi_1, \varphi_2)} = 0. \quad (32) \end{aligned}$$

Equation (31) is a generalized (or renormalized) Hartree

equation that incorporates phase correlations on the lattice into the mean-field description (5). The correlations are embodied in the direct component $v_d(\varphi)$ and the exchange potential $v_e(\varphi)$. They read

$$v_d(\varphi_1) = \sum_{\mathbf{n} \neq 0} \frac{1}{2\pi} \int_{-\pi}^{\pi} d\varphi_2 \rho(\varphi_2) g(\mathbf{n}; \varphi_1, \varphi_2) v_0(\mathbf{n}; \varphi_1, \varphi_2) \quad (33)$$

and

$$\begin{aligned} v_e(\varphi_1) = & \lambda \sum_{\mathbf{n} \neq 0} \frac{1}{2\pi} \int_{-\pi}^{\pi} d\varphi_2 \rho(\varphi_2) v_c(\mathbf{n}; \varphi_1, \varphi_2) \\ & - \frac{\lambda}{4} \sum_{\mathbf{m}} \frac{1}{2\pi} \int_{-\pi}^{\pi} d\varphi_3 \rho(\varphi_3) N'(\mathbf{m}; \varphi_1, \varphi_3) \\ & \times D(3) X'(\mathbf{m}; \varphi_3, \varphi_1). \quad (34) \end{aligned}$$

The Lagrange parameter μ ensures the unit-normalization of function $\sqrt{\rho(\varphi)}$. We note that the renormalized Hartree equation may be discarded for parameter values $\lambda > \lambda_c$, since the density profile is constant in the disordered phase. Equation (32) determines the site-site distribution function $g(\mathbf{n}; \varphi_1, \varphi_2)$ and is often called (in the theory of quantum fluids) a renormalized Schrödinger equation for the square root \sqrt{g} with zero-energy eigenvalue. It involves the induced potential

$$\begin{aligned} w(\mathbf{n}; \varphi_1, \varphi_2) = & -\frac{\lambda}{2} [D(1) + D(2)] N'(\mathbf{n}; \varphi_1, \varphi_2) \\ & - \frac{\lambda}{2} \sum_{\mathbf{m}} \frac{1}{2\pi} \int_{-\pi}^{\pi} d\varphi_3 \rho(\varphi_3) \\ & \times X'(\mathbf{n} - \mathbf{m}; \varphi_1, \varphi_3) D(3) X'(\mathbf{m}; \varphi_3, \varphi_2) \\ = & -\lambda D(1) N'(\mathbf{n}; \varphi_1, \varphi_2) - \frac{\lambda}{2} C(\mathbf{n}; \varphi_1, \varphi_2) \quad (35) \end{aligned}$$

with the quantity

$$\begin{aligned} C(\mathbf{n}; \varphi_1, \varphi_2) = & \sum_{\mathbf{m}} \frac{1}{2\pi} \int_{-\pi}^{\pi} d\varphi_3 \rho(\varphi_3) X'(\mathbf{n} - \mathbf{m}; \varphi_1, \varphi_3) \\ & \times D(3) X'(\mathbf{m}; \varphi_3, \varphi_2). \quad (36) \end{aligned}$$

For the purpose of numerical calculations it is convenient to use the HNC/0 scheme for a reformulation of Eq. (32) leading to the form

$$\begin{aligned} \lambda [D(1) + D(2)] X'(\mathbf{n}; \varphi_1, \varphi_2) - \lambda C(\mathbf{n}; \varphi_1, \varphi_2) \\ = -2V_{\text{ph}}(\mathbf{n}; \varphi_1, \varphi_2), \quad (37) \end{aligned}$$

wherein $V_{\text{ph}}(\mathbf{n}; \varphi_1, \varphi_2)$ is the particle-hole potential³²

$$V_{\text{ph}}(\mathbf{n}; \varphi_1, \varphi_2) = \dot{X}'(\mathbf{n}; \varphi_1, \varphi_2) - \frac{\lambda}{4} [D(1) + D(2)] X'(\mathbf{n}; \varphi_1, \varphi_2). \quad (38)$$

Function $\dot{X}'(\mathbf{n}; \varphi_1, \varphi_2)$ is a derivative of the direct component of a generalized distribution function $g(\mathbf{n}, \varphi_1, \varphi_2, \alpha)$ with respect to a parameter α . This function can be deter-

mined from a set of generalized HNC equations in which function $u(\mathbf{n}; \varphi_1, \varphi_2)$ is replaced by the modified pseudopotential^{25,26}

$$u(\mathbf{n}, \varphi_1, \varphi_2, \alpha) = u(\mathbf{n}; \varphi_1, \varphi_2) + \alpha v^*(\mathbf{n}; \varphi_1, \varphi_2). \quad (39)$$

Quantities g , X , and N are functions of the parameter α and the corresponding dot quantities can be determined from generalized HNC equations by taking the derivatives with respect to α at $\alpha=0$. The result provides the corresponding HNC dot equations. In HNC/0 approximation they reduce to

$$\dot{g}(0; \varphi_1, \varphi_2) \equiv 0, \quad (40)$$

$$\dot{g}(\mathbf{n}; \varphi_1, \varphi_2) = g(\mathbf{n}; \varphi_1, \varphi_2)[v^*(\mathbf{n}; \varphi_1, \varphi_2) + \dot{N}'(\mathbf{n}; \varphi_1, \varphi_2)], \quad (41)$$

$$\dot{X}'(\mathbf{n}; \varphi_1, \varphi_2) = \dot{g}(\mathbf{n}; \varphi_1, \varphi_2) - \dot{N}'(\mathbf{n}; \varphi_1, \varphi_2), \quad (42)$$

$$\begin{aligned} \dot{N}'(\mathbf{n}; \varphi_1, \varphi_2) &= \sum_{\mathbf{m}} \frac{1}{2\pi} \int_{-\pi}^{\pi} d\varphi_3 \rho(\varphi_3) \dot{X}'(\mathbf{n} - \mathbf{m}; \varphi_1, \varphi_3) \\ &\quad \times [X'(\mathbf{m}; \varphi_3, \varphi_2) + N'(\mathbf{m}; \varphi_3, \varphi_2)] \\ &+ \sum_{\mathbf{m}} \frac{1}{2\pi} \int_{-\pi}^{\pi} d\varphi_3 \rho(\varphi_3) X'(\mathbf{n} - \mathbf{m}; \varphi_1, \varphi_3) \\ &\quad \times [\dot{X}'(\mathbf{m}; \varphi_3, \varphi_2) + \dot{N}'(\mathbf{m}; \varphi_3, \varphi_2)]. \end{aligned} \quad (43)$$

V. NUMERICAL RESULTS AND DISCUSSION

The optimized correlated ground-state wave function and the corresponding ground-state energy can be explicitly determined by solving the set of coupled Eqs. (20)–(28), (31), (32), and (40)–(43). The numerical procedure of the iteration scheme is outlined in the Appendix. The solutions of the Euler-Lagrange equations permit, of course, the enumeration of the optimal gross quantities of interest associated with the ground state. Here we report on some of our numerical results for the functions and quantities related to the optimized correlated ground state of the system as a function of the interaction strength λ . Figure 3 shows the numerical results on the optimal on-site density $\rho(\varphi)$ as a function of the phase φ for various values of the coupling parameter λ . The probability density is sharply peaked at $\varphi=0$ for small coupling parameters ($0 \leq \lambda \ll \lambda_c$) and agrees with the mean-field result since the correlations vanish as $\lambda \rightarrow 0$. In this limit the phases (or rotor angles) on the lattice are alike and independent of the lattice sites. With increasing strength λ the probability distribution $\rho(\varphi)$ broadens and equals unity at (and above) the critical point $\lambda_c \approx 2.97$, where the phases are randomly distributed and equally probable.

Figure 4 depicts numerical results on the optimal site-site probability function $P(\mathbf{n}; \varphi_1, \varphi_2) = \rho(\varphi_1)\rho(\varphi_2)g(\mathbf{n}; \varphi_1, \varphi_2)$, for nearest neighbors at various values of the strength $\lambda < \lambda_c$ as function of the relative phase $\varphi = \varphi_1 - \varphi_2 = 2\varphi_1$ with $\varphi_1 + \varphi_2 = 0$. The function has a maximum for $\varphi=0$ where $\varphi_1 =$

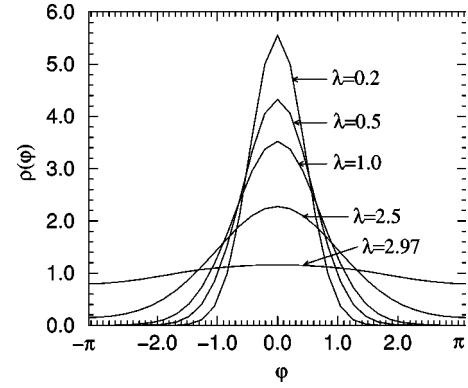


FIG. 3. The optimal on-site density profile $\rho(\varphi)$ calculated within the CBF theory for various values of the coupling parameter λ .

$-\varphi_2=0$. This means that—in spin interpretation—the orientation of the rotor axes at neighboring sites are parallel and pointing in the direction of the x axis. For $\varphi > 0$ this probability is rapidly decreasing.

Figure 5 represents numerical results on the optimal order parameter $M_x(\lambda)$ in the ordered phase of the O(2) model. Comparing with the mean-field data displayed in Fig. 1 we see a similar dependence of the CBF results for the order parameter M_x on the coupling strength λ , if we scale down this variable to a smaller value. At $\lambda=0$ function $\rho(\varphi)$ is proportional to a delta function $\delta(\varphi)$ and the order parameter M_x is unity. As λ increases the order parameter M_x decreases gradually due to the quantum phase fluctuations and drops continuously to zero at $\lambda_c = 2.97$, where these fluctuations become strong enough to destroy completely the long-range order forcing the system into the disordered phase for values $\lambda > \lambda_c$.

The results on the ground-state energy (Fig. 6) are significantly lower than those of mean-field theory displayed in Fig. 2 due to the negative correlation energy. This energy component vanishes, of course, at $\lambda=0$ and in the asymptotic limit $\lambda \rightarrow \infty$. The absolute value of the correlation energy is largest in the transition region amounting to about 10% of

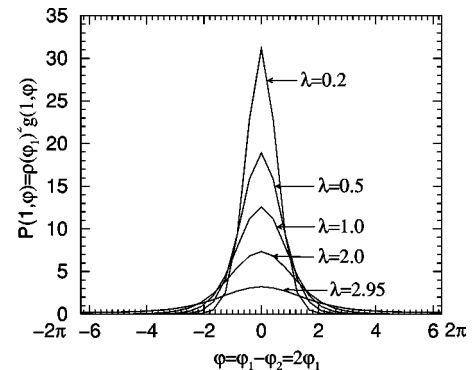


FIG. 4. The optimal site-site probability density $P(\mathbf{n}; \varphi_1, \varphi_2) = \rho(\varphi_1)\rho(\varphi_2)g(\mathbf{n}; \varphi_1, \varphi_2)$ for nearest neighbors as a function of relative angle $\varphi = \varphi_1 - \varphi_2$ (with $\varphi_1 + \varphi_2 = 0$, i.e., $\varphi = 2\varphi_1$) in the ordered phase, calculated within the CBF theory for various values of the coupling parameter λ .

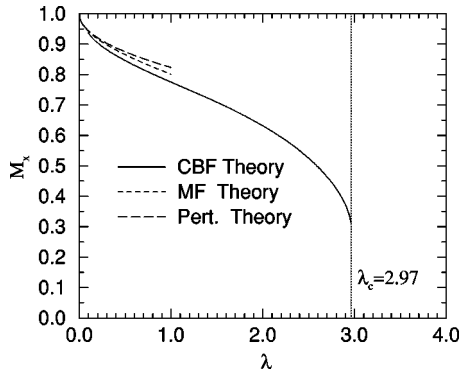


FIG. 5. CBF results for the order parameter M_x of the O(2) model on a simple square lattice. The parameter is nonzero in the ordered phase of the system, i.e., in the domain $0 \leq \lambda \leq \lambda_c \approx 2.97$. The dashed line and the long-dashed line show, respectively, the results of mean-field theory and of low-order perturbation theory.

the energy result in mean-field approximation. In the disordered phase, $\lambda > \lambda_c$, the CBF results on the energy are relatively close to the perturbation results based on the first-order expression (11).

Figures 7 and 8 display CBF results on the site-site distribution function $g(\mathbf{n}; \varphi_1, \varphi_2)$ for nearest neighbors. In the disordered regime of states (Fig. 7) the correlations depend only on the relative phase $\varphi = \varphi_1 - \varphi_2$. The function is plotted at three different values of the coupling parameter. Qualitatively, the dependence is essentially sinusoidal and becomes stronger with decreasing coupling parameter. The correlations are attractive for equal phase values ($\varphi=0$) and repulsive for a relative phase shift $\varphi=\pi$. Since the disordered states possess the full symmetry of the Hamiltonian, the distribution function has the symmetry $g(\mathbf{n}; \varphi) = g(\mathbf{n}; 2\pi - \varphi)$. This symmetry is broken in the ordered phase (Fig. 8). As a consequence, the phase correlations are strongest for $\varphi_1 = -\varphi_2 = \pi$ but are absent for $\varphi_1 = -\varphi_2 = 0$.

To analyze in more detail the spatial dependence of the correlations we may define a phase-averaged distribution function by³³

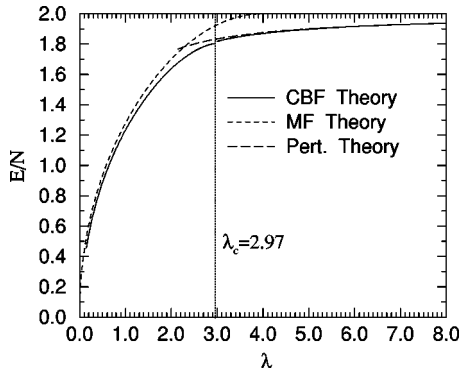


FIG. 6. CBF results on the ground-state energy per site for the O(2) model on a simple square lattice, as function of the coupling parameter λ . Displayed are also results of perturbation theory in lowest order (long-dashed line) and of mean-field theory (dashed line).

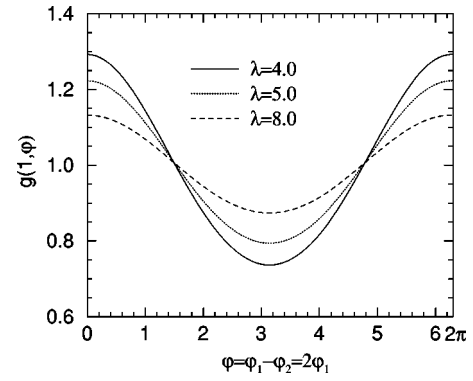


FIG. 7. Numerical results on the optimal site-site distribution function $g(\mathbf{n}; \varphi_1, \varphi_2)$ in CBF approximation, for nearest neighbors $|\mathbf{n}|=1$ in the disordered phase ($\lambda > \lambda_c \approx 2.97$), as function of $\varphi = \varphi_1 - \varphi_2$. In the disordered phase region this function depends only on the relative phase φ .

$$\begin{aligned}
 g(\mathbf{n}) &= \frac{\langle \Psi | \cos(\varphi_i - \varphi_j) | \Psi \rangle}{\langle \Psi | \Psi \rangle} \\
 &= \delta_{\mathbf{n},0} + \frac{1}{(2\pi)^2} \int_{-\pi}^{\pi} \int_{-\pi}^{\pi} d\varphi_1 d\varphi_2 \rho(\varphi_1) \\
 &\quad \times \rho(\varphi_2) g(\mathbf{n}; \varphi_1, \varphi_2) \cos(\varphi_1 - \varphi_2) \\
 &= \delta_{\mathbf{n},0} + G(\mathbf{n})|_{\mathbf{n} \neq 0}.
 \end{aligned} \tag{44}$$

For large distances ($|\mathbf{n}| \rightarrow \infty$) and in the weak-coupling limit ($\lambda \rightarrow \infty$) this function vanishes. It is long-ranged in the strong-coupling limit ($\lambda \rightarrow 0$) approaching the asymptotic value M_x^2 . It is therefore convenient to decompose this function (for $\mathbf{n} \neq 0$) into

$$G(\mathbf{n}) = M_x^2 + G_s(\mathbf{n}). \tag{45}$$

Function $G_s(\mathbf{n})$ is the short-ranged component of the correlation function, with the property $G_s(\infty) \rightarrow 0$. Figure 9 shows the CBF results for this function at different values of λ as a function of distance $|\mathbf{n}|$. It vanishes in the limits $\lambda \rightarrow 0$ and

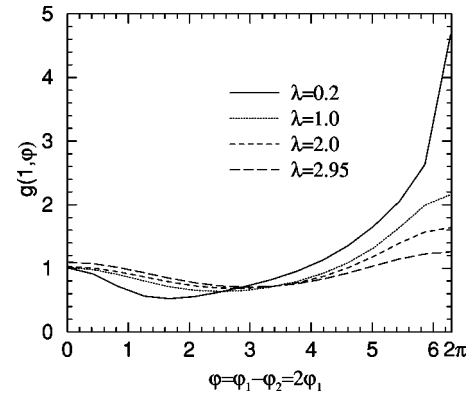


FIG. 8. Numerical results on the optimal site-site distribution function $g(\mathbf{n}; \varphi_1, \varphi_2)$ in CBF approximation, for nearest neighbors $|\mathbf{n}|=1$ as a function of $\varphi = \varphi_1 - \varphi_2 = 2\varphi_1$, in the ordered phase ($0 \leq \lambda < \lambda_c \approx 2.97$).

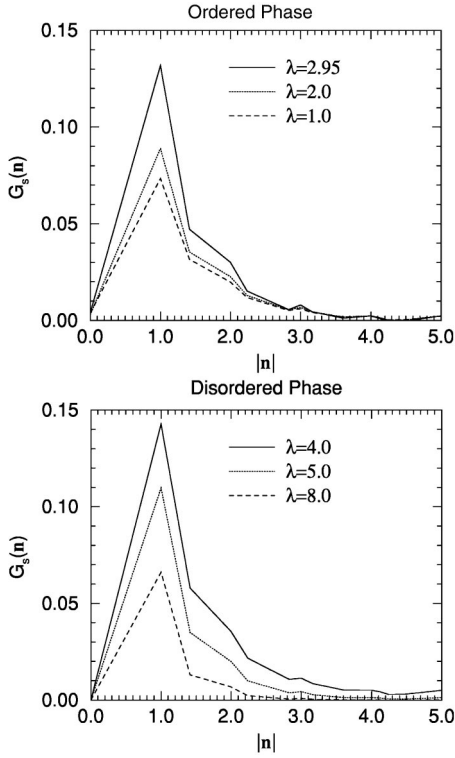


FIG. 9. The (short-ranged) averaged distribution function $G_s(\mathbf{n})$ as a function of relative distance $|\mathbf{n}|$, for various values of the coupling strength λ .

$\lambda \rightarrow \infty$ as we see from Fig. 9, where it increases as λ increases. It decreases above the critical strength λ_c . The dependence on the distance can be well matched by an exponential form of Yukawa type

$$G_s(\mathbf{n}) \approx \frac{G_0}{|\mathbf{n}|} e^{-\kappa|\mathbf{n}|}. \quad (46)$$

The parameter κ^{-1} may be interpreted as a correlation length. It approaches infinity if the system comes close to the critical point. We may calculate this correlation length via the relation $\ln[|\mathbf{n}|G_s(\mathbf{n})] = \ln G_0 - \kappa|\mathbf{n}|$ (Fig. 10).

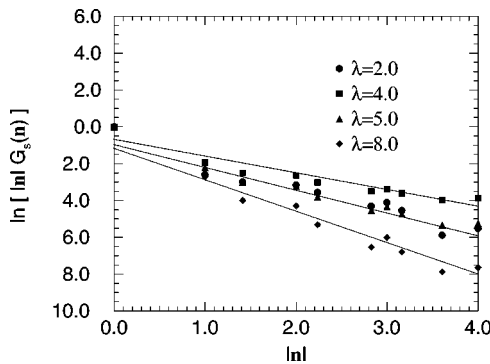


FIG. 10. The logarithm $\ln[|\mathbf{n}|G_s(\mathbf{n})]$ as a function of relative distance $|\mathbf{n}|$ for different values of the strength parameter λ . The inverse correlation length κ is determined by the slope of the curves.

VI. SUMMARY AND OUTLOOK

CBF theory has been adapted and employed for a detailed analysis of the O(2) model on a simple square lattice. Our main interest has been focused on a study of correlation effects in the ground state and their dependence on the strength of the coupling parameter that governs the ordering phenomena at zero temperature. We have explicitly constructed a pair-density functional for the ground-state energy in terms of the on-site density profile and the site-site distribution function that characterizes the existing correlations in the model system. Utilizing the minimum principle for the energy we derived, respectively, a renormalized Hartree equation for the optimal profile and a renormalized Schrödinger equation for the optimal site-site correlation function at zero eigenvalue. We designed an appropriate numerical procedure to solve these equations in conjunction with a set of HNC equations that permits to relate the pseudopotential and the Feenberg effective potential to the profile and the site-site distribution function (in HNC/0 approximation). On this variational level of the CBF theory the correlated N -body ground state of the O(2) lattice Hamiltonian is approximately represented by a Hartree-Jastrow wave function of optimal form. We note that the CBF theory provides a systematic scheme for improving the present approximation, at least in principle. Such improvements have been successfully performed in detailed studies of liquid helium with quantitative results of high numerical accuracy on spatial distribution functions, static and dynamic structure functions, a.o. CBF studies of lattice models on this more sophisticated level are feasible but are more complex and time consuming than in the case of liquid helium. Within the present realization of CBF theory we have calculated and discussed the optimal density profile, site-site distribution function, the ground-state energy, and the order parameter. Results are displayed in detail for the ordered phase (small coupling parameter) and in the disordered regime (large coupling parameter). The continuous phase transition occurs at a critical strength $\lambda_c \approx 2.97$. The correlations correct therefore the mean-field result by about 25%. They also lower the energy result of mean-field theory by about 10%. Afar from the transition region the correlations become less effective and disappear in the strong-coupling limit as well as in the weak-coupling regime. Approaching the critical region the correlations become long ranged. At present the analysis is not yet sufficiently developed to allow the extraction and evaluation of critical exponents at the transition point. Before attempting this rather ambitious task one should first turn to a number of interesting applications and some further developments.

The CBF formalism may be directly employed for semi-analytic studies of the ground-state properties of the O(2) model defined on three- or higher-dimensional lattices, for lattices with differing spatial symmetries, and more complex interactions that allow for frustration. With only marginal changes the CBF formalism can be implemented to analyze ground-state correlations in related lattice models, for example, correlations in chiral O(4) models, which are of interest in lattice meson-field theory.²⁹ One could further employ the CBF theory to investigate excited states of the O(2)

model or other lattice models at zero or finite temperatures^{34,35} in close formal analogy to CBF studies of quantum fluids³⁶ and of spin lattices.³⁷ Attempts in this direction are reported in Ref. 38.

Of particular interest would be a CBF analysis of topological excitations generated by the O(2) Hamiltonian in two spatial dimensions. Such a study may be performed in analogy to the CBF treatment of a single vortex and of a vortex-antivortex pair in two-dimensional liquid helium.^{39,40} One assumes that a vortex is a mobile (or trapped) quasiparticle with a mass self-consistently determined within the CBF theory. The corresponding correlated wave function is represented as a product of a many-body trial function of Jastrow type such as expression (13) (or, more generally, of Jastrow-Feenberg type) and a quantized complex phase factor [cf. Eq. (5) of Ref. 40]. On the same level of approximation the CBF state of a vortex-antivortex pair involves two complex phase factors corresponding to the two centers of circulation [cf. Eq. (16) of Ref. 40]. Based on these Ansatzes Refs. 39 and 40 report numerical results on the associated excitation energies, the vortex-antivortex interaction, and the chemical potential required to create a vortex-antivortex pair in a two-dimensional helium fluid. The present analysis of ground-state properties of the O(2) model could be extended to a formal and numerical study of topological excitations in lattice systems by a suitable adaptation of the formalism of Refs. 39 and 40. This adaptation can be done without major difficulties. However, numerical calculations will be more extensive for the lattice O(2) model than for the homogeneous helium phase, since in the former case one has to deal with angular-dependent one-body densities (15).

ACKNOWLEDGMENTS

Part of this work was done at the Max-Planck Institut für Physik Komplexer Systeme, Dresden, Germany. K.A.Q. thanks for the kind hospitality and acknowledges financial support from this Institut and the “Deutscher Akademischer Austauschdienst.”

APPENDIX: NUMERICAL PROCEDURE

Numerical evaluation of the relevant solutions of the Euler-Lagrange Eqs. (31) and (32) at given parameter λ is essentially done by appropriate iteration procedures. We begin with a suitably chosen input for the (as yet unknown) pseudopotential. In this initial step we adopt a simple form $u(\mathbf{n}; \varphi_1, \varphi_2) = \gamma \Delta(\mathbf{n})$. The parameter γ is determined by minimizing the energy functional within the adopted HNC/0 approximation. We then determine the corresponding one-body density profile by solving the renormalized Hartree Eq. (31), employing a Newton-Raphson algorithm. Next, the HNC/0 equations are solved by matrix inversion and iteration. The optimal parameter form for the pseudopotential is then used as an input to solve the full set of coupled equations simultaneously. For this purpose it is advisable to reformulate the

two-body integrodifferential Eq. (37). Multiplication of this equation by $\sqrt{\rho(\varphi_1)\rho(\varphi_2)}$ leads to the more convenient form

$$\begin{aligned} \lambda[H_0(1) + H_0(2)]\tilde{X}'(\mathbf{n}; \varphi_1, \varphi_2) \\ = \lambda\tilde{C}(\mathbf{n}; \varphi_1, \varphi_2) - 2\tilde{V}_{ph}(\mathbf{n}; \varphi_1, \varphi_2). \end{aligned} \quad (\text{A1})$$

The operator $H_0(i)$ in Eq. (A1) is defined by

$$\begin{aligned} H_0(i) &= -\frac{1}{\sqrt{\rho(\varphi_i)}} \frac{\partial}{\partial \varphi_i} \rho(\varphi_i) \frac{\partial}{\partial \varphi_i} \frac{1}{\sqrt{\rho(\varphi_i)}} \\ &= -\frac{\partial^2}{\partial \varphi_i^2} + \frac{1}{\sqrt{\rho(\varphi_i)}} \frac{\partial^2 \sqrt{\rho(\varphi_i)}}{\partial \varphi_i^2} \\ &= -\frac{\partial^2}{\partial \varphi_i^2} + \frac{1}{\lambda} \mathcal{F}(\varphi_i), \end{aligned} \quad (\text{A2})$$

where $\mathcal{F}(\varphi)$ is obtained from Eq. (31):

$$\mathcal{F}(\varphi) = v_d(\varphi) + v_e(\varphi) - \mu. \quad (\text{A3})$$

The tilde quantity $\tilde{f}(\mathbf{n}; \varphi_1, \varphi_2)$ is defined as

$$\tilde{f}(\mathbf{n}; \varphi_1, \varphi_2) = \sqrt{\rho(\varphi_1)\rho(\varphi_2)} f(\mathbf{n}; \varphi_1, \varphi_2). \quad (\text{A4})$$

Explicitly, quantity $\tilde{C}(\mathbf{n}; \varphi_1, \varphi_2)$ is given by

$$\begin{aligned} \tilde{C}(\mathbf{n}; \varphi_1, \varphi_2) &= \sum_{\mathbf{m}} \frac{1}{2\pi} \int_{-\pi}^{\pi} d\varphi_3 \tilde{X}'(\mathbf{n} - \mathbf{m}; \varphi_1, \varphi_3) \\ &\quad \times H_0(3) \tilde{X}'(\mathbf{m}; \varphi_3, \varphi_2) \\ &= \sum_{\mathbf{m}} \frac{1}{2\pi} \int_{-\pi}^{\pi} d\varphi_3 \partial_{\varphi_3} \tilde{X}'(\mathbf{n} - \mathbf{m}; \varphi_1, \varphi_3) \\ &\quad \times \partial_{\varphi_3} \tilde{X}'(\mathbf{m}; \varphi_3, \varphi_2) \\ &\quad + \frac{1}{\lambda} \sum_{\mathbf{m}} \frac{1}{2\pi} \int_{-\pi}^{\pi} d\varphi_3 \tilde{X}'(\mathbf{n} - \mathbf{m}; \varphi_1, \varphi_3) \\ &\quad \times \mathcal{F}(\varphi_3) \tilde{X}'(\mathbf{m}; \varphi_3, \varphi_2). \end{aligned} \quad (\text{A5})$$

Next, we solve the HNC/0 dot equations and determine the function $\tilde{X}'(\mathbf{n}; \varphi_1, \varphi_2)$ and the function $V_{ph}(\mathbf{n}; \varphi_1, \varphi_2)$ via Eq. (38). The two-body Eq. (37) is solved using a finite-difference relaxation method⁴¹ and by iteration. We replace the derivative by a finite-difference defined on an $n \times n$ lattice in φ space with $n=31$ and construct the sparse matrix. After converting the two-dimensional matrix into a one-dimensional array and splitting the sparse matrix into two components—a rest matrix and an invertible one—we iterate and achieve rapid convergence. In each step of the adopted iteration we determine new functions $X'(\mathbf{n}; \varphi_1, \varphi_2)$ and $N'(\mathbf{n}; \varphi_1, \varphi_2)$ and therewith a new correlation function $u^{\text{new}}(\mathbf{n}; \varphi_1, \varphi_2)$ for $\mathbf{n} \neq 0$ via the construct

$$u^{\text{new}}(\mathbf{n}; \varphi_1, \varphi_2) = \ln[g^{\text{new}}(\mathbf{n}; \varphi_1, \varphi_2) - N'^{\text{new}}(\mathbf{n}; \varphi_1, \varphi_2)]. \quad (\text{A6})$$

Finally we determine the optimal on-site density profile, the optimal site-site correlation function, and other physical quantities of interest. To perform the analogous calculations

at other values of the strength parameter λ we discretise the parameter interval by steps $\Delta\lambda=0.01$. With the optimal solutions derived for λ as input quantities we employ the same numerical technique to calculate the optimal functions and other data at strength parameter $\lambda+\Delta\lambda$.

*Electronic address: kq@mpipks-dresden.mpg.de

†Electronic address: ristig@thp.uni-koeln.de

¹C. J. Hamer, J. B. Kogut, and L. Susskind, Phys. Rev. D **19**, 3091 (1979).

²C. Rojas and J. V. José, Phys. Rev. B **54**, 12 361 (1996).

³L. Amico and V. Penna, Phys. Rev. B **62**, 1224 (2000).

⁴D. Dalidovich and P. Phillips, Phys. Rev. B **59**, 11 925 (1999).

⁵M. V. Simkin, Phys. Rev. B **44**, 7074 (1991).

⁶T. K. Kopeć and J. V. José, Phys. Rev. B **63**, 064504 (2001).

⁷E. Šimánek, *Inhomogeneous Superconductors* (Oxford University Press, Oxford, 1994).

⁸S. Katsumoto, J. Low Temp. Phys. **98**, 287 (1995).

⁹H. S. J. van der Zant, W. J. Elion, L. J. Geerligs, and J. E. Mooij, Phys. Rev. B **54**, 10 081 (1996).

¹⁰M. P. A. Fisher, P. B. Weichman, G. Grinstein, and D. S. Fisher, Phys. Rev. B **40**, 546 (1989).

¹¹S. Doniach, Phys. Rev. B **24**, 5063 (1981).

¹²D. Ariosa and H. Beck, Phys. Rev. B **45**, 819 (1992).

¹³G. Grignani, A. Mattoni, P. Sodano, and A. Trombettoni, Phys. Rev. B **61**, 11 676 (2000).

¹⁴E. Šimánek, Solid State Commun. **31**, 419 (1979).

¹⁵D. M. Wood and D. Stroud, Phys. Rev. B **25**, 1600 (1982).

¹⁶K. B. Efetov, Zh. Eksp. Teor. Fiz. **78**, 2017 (1980) [Sov. Phys. JETP **51**, 1015 (1980)].

¹⁷E. Šimánek, Phys. Rev. B **32**, 500 (1985).

¹⁸R. S. Fishman, Phys. Rev. B **42**, 1985 (1990).

¹⁹W. Wang, Doctoral thesis, Universität zu Köln (Shaker Verlag, Aachen, 1997).

²⁰B. J. Kim, J. Kim, S. Y. Park, and M. Y. Choi, Phys. Rev. B **56**, 395 (1997).

²¹L. Jacobs, J. V. José, M. A. Novotny, and A. M. Goldman, Phys. Rev. B **38**, 4562 (1988).

²²J. Mikalopas, M. Jarrel, F. J. Pinski, W. Chung, and M. A. Novotny, Phys. Rev. B **50**, 1321 (1994).

²³T. K. Kopeć and J. V. José, Phys. Rev. B **60**, 7473 (1999).

²⁴J. W. Clark and E. Feenberg, Phys. Rev. **113**, 388 (1959).

²⁵E. Feenberg, *Theory of Quantum Fluids* (Academic Press, New

York, 1969).

²⁶E. Krotscheck, in *Microscopic Quantum Many-Body Theories and Their Applications*, Lecture Notes in Physics Vol. 510, edited by J. Navarro and A. Polls (Springer, Berlin, 1998), p. 187.

²⁷A. Dabringhaus, M. L. Ristig, and J. W. Clark, Phys. Rev. D **43**, 1978 (1991).

²⁸M. L. Ristig and J. W. Kim, Phys. Rev. B **53**, 6665 (1996).

²⁹R. F. Bishop, N. E. Ligterink, and N. R. Walet, in *Condensed Matter Theories*, edited by D. J. Ernst, I. E. Perakis, and A. S. Umar (Nova Science Publishers, Huntington, New York, 2000), Vol. 14.

³⁰K. A. Gernoth and J. W. Clark, J. Low Temp. Phys. **96**, 153 (1994).

³¹K. Abu Qasem, Doctoral thesis, Universität zu Köln, 2002.

³²E. Krotscheck, G.-X. Qian, and W. Kohn, Phys. Rev. B **31**, 4245 (1985).

³³W. Wang and M. L. Ristig, Phys. Lett. A **241**, 122 (1998).

³⁴G. Senger, M. L. Ristig, K. E. Kürten, and C. E. Campbell, Phys. Rev. B **33**, 7562 (1986).

³⁵T. Lindenau, M. L. Ristig, J. W. Clark, and K. A. Gernoth, J. Low Temp. Phys. **129**, 143 (2002).

³⁶L. Szybisz and M. L. Ristig, Phys. Rev. B **40**, 4391 (1989).

³⁷M. L. Ristig, J. W. Kim, and J. W. Clark, in *Theory of Spin and Lattice Gauge Models*, Lecture Notes in Physics Vol. 494, edited by J. W. Clark and M. L. Ristig (Springer-Verlag, Berlin, 1997).

³⁸M. L. Ristig, K. Abu Qasem, D. J. J. Farnell, and K. E. Kuerten, BgNS Transactions **7**, 145 (2002).

³⁹M. Saarela and F. Kusmartsev, in *Condensed Matter Theories*, edited by L. Blum and F. B. Malik (Plenum Press, New York, 1993), Vol. 8.

⁴⁰M. Saarela, B. E. Clements, E. Krotscheck, and F. V. Kusmartsev, in *Condensed Matter Theories*, edited by M. Casas, M. de Llano, J. Navarro, and A. Polls (Nova Science Publishers, Commack, NY, 1995), Vol. 10.

⁴¹W. H. Press, B. P. Flannery, S. A. Teukolsky, and W. T. Vetterling, *Numerical Recipes* (University Press, Cambridge, 1986), Chap. 19.